Applied Catalysis B: Environmental 147 (2014) 879–887

Contents lists available at ScienceDirect

Applied Catalysis B: Environmental

journal homepage: www.elsevier.com/locate/apcatb

CoMo/SBA-15 catalysts prepared with EDTA and citric acid and their performance in hydrodesulfurization of dibenzothiophene

Laura Peña, Diego Valencia*, Tatiana Klimova

Facultad de Química, Universidad Nacional Autónoma de México, Cd. Universitaria, Coyoacán, México D.F. 04510, Mexico

ARTICLE INFO

Article history:
Received 23 June 2013
Received in revised form 6 October 2013
Accepted 9 October 2013
Available online 18 October 2013

Keywords:
CoMo catalysts
SBA-15
EDTA
Citric acid
Hydrodesulfurization

ABSTRACT

A series of CoMo catalysts supported on SBA-15 were prepared with ethylenediaminetetraacetic acid (EDTA) and citric acid (CA) as chelating agents. The catalysts were prepared varying the MoO_3 charges (6, 12 and 18 wt.%). They were characterized by several techniques (N_2 physisorption, powder and small-angle XRD, TPR, DRS and HRTEM) and tested in hydrodesulfurization (HDS) of dibenzothiophene (DBT). The catalysts prepared without chelating agents showed a crystalline phase (β-$CoMoO_4$) since the lowest metal charge, detected by powder XRD. The addition of chelating agents in the impregnation solution avoided the precipitation of this crystalline phase on the SBA-15 surface. HRTEM measurements exhibited smaller MoS_2 particles when the catalysts were prepared with chelating agents. Highly active catalysts were synthesized with EDTA and CA. The increase in the metal charges in the CoMo/SBA-15 catalysts without chelating agents resulted in little increment in the catalytic activity. However, the catalytic activity showed an important enhancement when the metal species were impregnated in presence of EDTA or CA.

1. Introduction

Combustion of gasoline and diesel obtained from crude oils with large amount of sulfur-, nitrogen- and oxygen-containing compounds produces SO_x, NO_x that pollute atmosphere and lead to corrosion of reactors and storage vessels [1,2]. Particularly, the heteroaromatic compounds are difficult to eliminate because the larger compounds stability [3]. Environmental regulations require the reduction of sulfur content in fuels. The process to accomplish this aim has been hydrodesulfurization (HDS), which is a reaction of fluid phase with hydrogen in presence of heterogeneous catalyst at high temperature and pressure [4]. S-containing aromatic compounds are less reactive in the HDS process. Typically, HDS catalysts are MoS_2 crystallites promoted by CoS or NiS and supported on a stable oxide material such as γ-Al_2O_3. In order to improve the common catalyst activity, there are some advances in the preparation process. One of them is a modification in the catalysts' components such as replacement of the support for a high specific surface oxide such as the mesoporous silica. Unfortunately, the interaction between SiO_2 and Mo species is very weak; this affects the dispersion of sulfided active phase [5]. For this fact and the high calcination temperature, the formation of β-$CoMoO_4$ crystalline phase has been observed in the CoMo/SBA-15 catalysts [6–8]. It is sulfided a very high temperature and it has low activity, so that it is an undesirable effect in HDS catalysts [9]. Some modifications of silica have been developed to increase the metal–support interactions, *e.g.*, ZrO_2, TiO_2 grafting of SiO_2 resulted in a high dispersion of active phase and the highly active and selective CoMo catalysts especially for HDS of the refractory polyaromatic sulfur compounds [6–8].

Another key to produce highly active catalysts for HDS, at the preparation stage, is the modification of the metal species in the impregnation solution. There are several ways to change those species and it has consequences in their catalytic performance. Chelating agents have been used for preparing HDS catalysts with good results [10]. Several studies try to determinate their effects in HDS catalysts. Nitrilotriacetic acid (NTA), ethylenediaminetetraacetic acid (EDTA) and 1,2-cyclohexanediamine-N,N,N′,N′-tetraacetic acid (CyDTA) have been proved in the preparation of HDS catalysts. The results showed an increase in the activity in HDS of benzothiophene (BT) with the following order CyDTA > EDTA > NTA and the authors account an effective formation of highly active sites [11].

Chelating agents as diammonium salt of ethylenediaminetetraacetate (diA-EDTA) renders soluble β-$CoMoO_4$ phase in CoMo catalysts [12]. It is evident that chelating agents can prevent the formation of this phase. IR spectroscopy of adsorbed CO demonstrates the presence of EDTA during the preparation of CoMo catalysts increases the amount of CoMoS sites without modifying the amount of unpromoted MoS_2 sites, thus the total sites increases with EDTA

* Corresponding author. Tel. +52 5556223522.
E-mail address: dvalencia@comunidad.unam.mx (D. Valencia).

0926-3373/$ – see front matter © 2013 Elsevier B.V. All rights reserved.
http://dx.doi.org/10.1016/j.apcatb.2013.10.019

[13]. The promotion of these CoMoS sites plays an important role in their catalytic performance in HDS of S-containing compounds [14] CoMo catalysts prepared with chelating agents had better catalytic performance when they were not calcined before sulfidation [15]. In this case, better promotion of CoMoS phase was observed [16]. Most of the above studies have been performed in HDS of thiophene or hydrogenation reactions of alkenes. However, when CoMo-NTA catalyst supported on γ-Al_2O_3 was tested in HDS of dibenzothiophene (DBT), one of the refractory model molecules of gasoline and diesel fuels, no changes in activity neither in selectivity were detected [17].

CoMo catalysts supported on Al_2O_3 or alumina modified with zeolites were found to be active to desulfurize refractory compounds such as DBT and 4,6-dimethyldibenzothiophene (4,6-DMDBT). CoMoP catalyst prepared with citric acid (CA) and supported on HY-Al_2O_3 was one of the attractive system [18]. CA added to this catalyst increased its activity considerably using commercial diesel, this effect is related to dispersion and sulfidation temperature [19]. This catalyst diminished the sulfur content below 16 ppm of S and had some advantages in resistance to presence of N-containing compounds reaching elimination of N below 5 ppm at 350 °C. The optimal temperature for the thermal treatment of this catalyst before sulfidation stage was up to 100 °C. At higher temperatures (between 300–500 °C) rate constant decreased [20]. CA was also used in the preparation of CoMo/γ-Al_2O_3 catalysts modified with boron. Addition of CA increased the dispersion of Co and Mo species, resulting in a larger amount of Co—Mo—S after sulfidation, without active-site blocking by cobalt sulfide clusters [21].

EDTA and CA have been used for preparing NiMo catalysts supported on SBA-15 with remarkable results in HDS [22,23]. CA showed a modification of the catalytically active sites depending on the preparation conditions [24,25]. These catalysts were highly active when they were calcined because the hydrogenation route is favored. CoMo/SBA-15 catalysts have not been prepared with chelating agents for HDS. In the present work, we synthesized a series of CoMo catalysts supported on SBA-15 with EDTA and CA. The MoO_3 and CoO charges for these catalysts were varying to get insight into effect of both chelating agents in dispersion of metal species and their catalytic performance in HDS of DBT.

2. Experimental

2.1. Preparation of support and catalysts

The pure silica SBA-15 material with *p6mm* hexagonal structure was synthesized according to well-known procedure using the triblock copolymer P123 ($EO_{20}PO_{70}EO_{20}$, M_{av} = 5800, Aldrich) as the structure directing agent and tetraethyl orthosilicate (TEOS, Aldrich, 99.999%) as silica source [26,27]. 4 g of triblock copolymer P123 was dissolved in 30 g of water and 120 g of 2 M HCl solution at 35 °C. Then 8.5 g of TEOS was added into the solution. The solution was stirred at 35 °C for 20 h and aged at 80 °C for 48 h without stirring. The solid product was collected by filtration, washed with deionized water and air-dried at room temperature. Then, the solid product was calcinated in static air at 550 °C during 6 h.

Three CoMo/SBA-15 catalysts series were prepared by coimpregnation of ammonium heptamolybdate, $(NH_4)_6Mo_7O_{24}{\cdot}4H_2O$ (Merck, 99%), and cobalt nitrate, $Co(NO_3)_2{\cdot}6H_2O$ (Baker, 99.1%), in presence of ethylenediaminetetraacetic acid, $C_{10}H_{16}N_2O_8$ (Aldrich, 99.995%), or citric acid, $C_6H_8O_7{\cdot}H_2O$ (Merck, 99.5%). Catalysts without chelating agents were also prepared with the same procedure. The calcined SBA-15 support was impregnated using these solutions in each case. Nominal metal charges of the catalysts are shown in Table 1, the molar ratio Co:EDTA = 1:1 and Co:CA = 1:2 were kept to form its respective coordination compound. This stoichiometry was also used because it exhibited better catalytic performance for MoS_2-based catalysts in HDS of DBT [28]. The catalysts were denoted as CoMo(x) or CoMo(x)(y) where $x = MoO_3$ wt.%. and y = E (EDTA) or C (CA). The pH of impregnation solution was adjusted with ammonia solution to get pH = 9 for the catalysts prepared with EDTA or CA. CoMo/SBA-15 catalysts were dried first at room temperature for 12 h, then at 100 °C for 24 h and finally, they were calcined at 500 °C for 4 h under air atmosphere.

2.2. Characterization of catalysts

The SBA-15 support and catalysts were characterized by N_2 physisorption, powder X-ray diffraction (XRD) and small-angle XRD. The catalysts were also characterized by UV–vis diffuse reflectance spectroscopy (DRS), temperature-programmed reduction (TPR) and high resolution transmission electron microscopy (HRTEM). N_2 adsorption–desorption isotherms were measured with a Micromeritics ASAP 2000 automatic analyzer at liquid N_2 temperature. Prior to the experiments, the samples were degassed ($p < 10^{-1}$ Pa) at 270 °C for 6 h. Specific surface area was calculated by the BET method (S_{BET}), the total pore volume (V_p) was determinate by nitrogen adsorption at a relative pressure of 0.98 and pore size distribution from the desorption isotherm by the BJH method. The mesopore diameter (D_p) corresponds to the maximum of the pore size distribution. The micropore area (S_μ) was estimated using the correlation of t-Harkins & Jura (t-plot method). XRD patterns were recorded in $3^\circ \leq 2\theta \leq 60^\circ$ range on a Siemens D5000 diffractometer, using Cu Kα radiation (λ = 1.5406 Å) and a goniometer speed of 1° (2θ) min^{-1}. Small-angle XRD (2θ = 1–10°) was performed on a Bruker D8 Advance diffractometer using small divergence and scattering slits of 0.05°. The a_0 unit-cell parameter was estimated from the position of the (1 0 0) diffraction line ($a_0 = d_{100} \times 2/\sqrt{3}$) [29]. Pore wall thickness (δ), was assessed by subtracting D_p from to a_0 unit-cell parameter which corresponds to the distance between the centers of adjacent mesopores. UV–vis electronic spectra of the samples were recorded in the wavelength range 200–800 nm using a Varian Cary 100 spectrophotometer equipped with a diffuse reflectance attachment. Polytetrafluoroethylene was used as a reference. TPR experiments were carried out in Micromeritics Auto Chem II 2920 automatic analyzer equipped with a TC detector. The samples were pretreated *in situ* at 400 °C for 2 h under air flow and cooled in Ar stream. The reduction step was performed under a stream of an Ar/H_2 mixture (90/10 mol/mol and 50 ml min^{-1}), with a heating rate of 10 °C min^{-1} up to 1000 °C. HRTEM measurements were performed using Jeol 2010 microscope (resolving power 1.9 Å). The sulfided catalysts were ultrasonically dispersed in *n*-heptane and the suspension was collected on carbon-coated grids. Slab length and layer stacking distributions of MoS_2 crystallites in each sample were established from the measurement of at least 300 crystallites detected on several HRTEM micrographs taken from different parts of the same sample dispersed on the microscope grid.

2.3. Catalytic activity

The DBT HDS tests were performed in a batch reactor at 300 °C and 7.3 MPa total pressure for 8 h. Before the catalytic activity testing, the catalysts were sulfided *ex situ* in a tubular reactor at 400 °C for 4 h in a stream of 15 vol.% of H_2S/H_2 under atmospheric pressure. The sulfided catalysts (0.15 g) were transferred in an inert atmosphere (Ar) to a batch reactor (Parr) with 40 ml of *n*-hexadecane solution containing 0.054 mol L^{-1} (2160 ppm of S) of DBT. The reaction was followed by withdrawing aliquots each hour. To corroborate product identification, the product mixture was analyzed on a Hewlett Packard GC MS instrument.

Table 1
Notation, textural and structural characteristics of support and the CoMo catalysts supported on SBA-15.

Sample	MoO_3 (wt.%)	CoO (wt.%)	Chelating agent	S_{BET} ($m^2\,g^{-1}$)	S_μ[a] ($m^2\,g^{-1}$)	V_p ($cm^3\,g^{-1}$)	D_p[b] (Å)	a_0[c] (Å)	δ[d] (Å)
SBA-15	–	–	–	775	103	1.05	60	111	51
CoMo6	6	1.5	–	662	94	0.97	54	112	58
CoMo12	12	3	–	581	82	0.84	55	113	58
CoMo18	18	4.5	–	551	68	0.81	57	114	58
CoMo6E	6	1.5	EDTA	529	54	0.90	54	113	59
CoMo12E	12	3	EDTA	483	57	0.81	54	113	59
CoMo18E	18	4.5	EDTA	442	46	0.75	55	114	59
CoMo6C	6	1.5	CA	543	64	0.95	54	111	57
CoMo12C	12	3	CA	471	54	0.82	53	112	59
CoMo18C	18	4.5	CA	435	53	0.74	53	113	60

[a] Micropore area.
[b] Pore diameter determined from the desorption isotherms by the BJH method.
[c] Unit-cell parameter estimated from the position of the (1 0 0) diffraction line ($a_0 = d_{100} \times 2/\sqrt{3}$).
[d] Pore wall thickness ($\delta = a_0 - D_p$).

3. Results and discussion

3.1. Characterization of catalysts

The textural characteristics of SBA-15 support and catalysts are shown in Table 1. The SBA-15 support presents a textural characteristic such as specific surface area of 775 $m^2\,g^{-1}$, micropore area of 103 $m^2\,g^{-1}$ and total pore volume of 1.05 $cm^3\,g^{-1}$. The textural characteristics of CoMo catalysts are smaller than the ones for SBA-15 support, these features decrease with increasing nominal metal charges. The catalytic materials showed lower values on their textural characteristics as the metal charges increase, these are expected due to the incorporation of larger charges of metal species on the support surface. CoMo(x)E and CoMo(x)C catalysts showed also a decrease in their textural characteristics than CoMo(x) catalysts with the same charge, the micropore area and total pore volume follow a similar trend. The pore diameter maintains similar values in all samples. The decrease in the textural characteristics of the CoMo(x)E and CoMo(x)C materials could be attributed to a little incorporation of chelating agents. Fig. 1 shows the N_2 adsorption–desorption isotherms of SBA-15 support, CoMo6(y), CoMo12(y) and CoMo18(y) catalysts. The shape of N_2 adsorption–desorption isotherm did not suffer an important change after catalyst preparation. All of them are type IV and have an H1 hysteresis loop, the addition of chelating agents does not produce changes in the isotherms shape. Small-angle XRD patterns of SBA-15 support, CoMo6(y), CoMo12(y) and CoMo18(y) catalysts are shown in Fig. 2, these exhibit three well-defined peaks indexed as (100), (110) and (200), corresponding of well-known *p6mm* hexagonal pore symmetry of SBA-15 support. The position of the reflections does not change after chelating agents addition, this indicate that the long-range periodicity of SBA-15 is intact. In addition, the unit-cell parameter of SBA-15 has a similar value compared with the catalysts (Table 1). The calculations of pore wall thickness are shown in Table 1. The results of N_2 physisorption and small-angle XRD indicate that the use of EDTA and CA, as chelating agents, and the preparation conditions do not modify the hexagonal pore symmetry of SBA-15 for all the metal charges studied.

Powder X-ray diffraction patterns of SBA-15, CoMo6(y), CoMo12(y) and CoMo18(y) catalysts in the 2θ range from 5° to 60° are shown in Fig. 3. The XRD pattern of SBA-15 has a long signal in the 15° and 35° associated to the amorphous silica. CoMo/SBA-15 catalysts prepared without chelating agents exhibited the formation of a crystalline phase. This signal reveals the formation of β-$CoMoO_4$ phase (JCPDS card 21-868) since low metal charges. Similar results have been reported for CoMo catalysts supported on SBA-15 [6–8,30]. The metal agglomeration in these catalysts is an undesirable effect. XRD patterns of CoMo(x)E and CoMo(x)C catalysts do not exhibit the reflections of the β-$CoMoO_4$ phase. Furthermore, the use of EDTA and CA during the impregnation of the metal species to the support inhibited the formation of the β-$CoMoO_4$ crystalline phase. It implies a good dispersion of the Mo and Co species in the CoMo(x)E and CoMo(x)C catalysts. Both chelating agents avoid the agglomeration of Co–Mo species on the SBA-15 surface since 6 wt.% MoO_3, the EDTA and CA compounds increases the metal dispersion. The use of both chelating agents stabilizes the impregnation solution to prevent the precipitation of Co–Mo species on SBA-15. The Co-complexes synthesized with EDTA and CA are very stable compared to the $[Co(H_2O)_6]^{2+}$ ion and prevent the formation of the $Co(OH)_2$, an insoluble compound. The Mo(VI) equilibrium also suffers a modification, the MoO_4^{2-} soluble specie is formed instead of the $Mo_7O_{24}^{6-}$ in the impregnation solutions with both chelating agents [31]. Furthermore, the chelating agents modify metal species in the impregnation solution and the interaction with support to the better dispersion of metal species on SBA-15.

UV–vis diffuse reflectance spectra (DRS) of CoMo6(y) and CoMo12(y) catalysts are shown in Fig. 4. The absorption bands corresponding to ligand-to-metal charge transfer (LMCT) $O^{2-} \rightarrow Mo^{6+}$ can be observed in the 200–360 nm region. The exact position of the bands reflects the local symmetry around the Mo^{6+} depending on their coordination and aggregation state [32]. The catalysts have two characteristic absorption bands, the first one is at about 220 nm and the second one is at ~250 nm. The absorption band about 220 nm is a mixture between molybdate species in Oh and Td symmetry. The absorption band at ~250 nm corresponding to isolated molybdate species in tetrahedral coordination, this band is well observed in all CoMo/SBA-15 catalysts. Both types of Mo^{6+} species can be observed in all catalysts, but are well defined in CoMo(x)E and CoMo(x)C ones. The changes on DR spectra of CoMo(x)E and CoMo(x)C catalysts could be attributed to an increase in the proportion of dispersed octahedral Mo species by the modification due to EDTA and CA. The electronic absorption intensity of the CoMo/SBA-15 catalysts increases as the metal content increases.

TPR profiles of the CoMo catalysts (Fig. 5) exhibited hydrogen consumption in a broad temperature range (between 400 °C and 800 °C). The main reduction peaks of these catalysts can be attributed to the first step of Mo reduction ($Mo^{6+} + 2e^- \rightarrow Mo^{4+}$) of polymeric octahedral species weakly bound to the SBA-15 support and the high temperature peak is associated with complete reduction ($Mo^{4+} + 4e^- \rightarrow Mo^0$) of polymeric octahedral, tetrahedral and bulk crystalline MoO_3 [33]. The main reduction peak for the CoMo/SBA-15 catalysts without chelating agents appears at higher temperature than the ones prepared with chelating agents for all the metal charges studied. For instance, the CoMo6 catalyst showed a main reduction peak around 488 °C, whereas the main reduction peaks for CoMo6E and CoMo6 C are 474 °C and 484 °C, respectively. The increase on the metal charges resulted in a modification in the

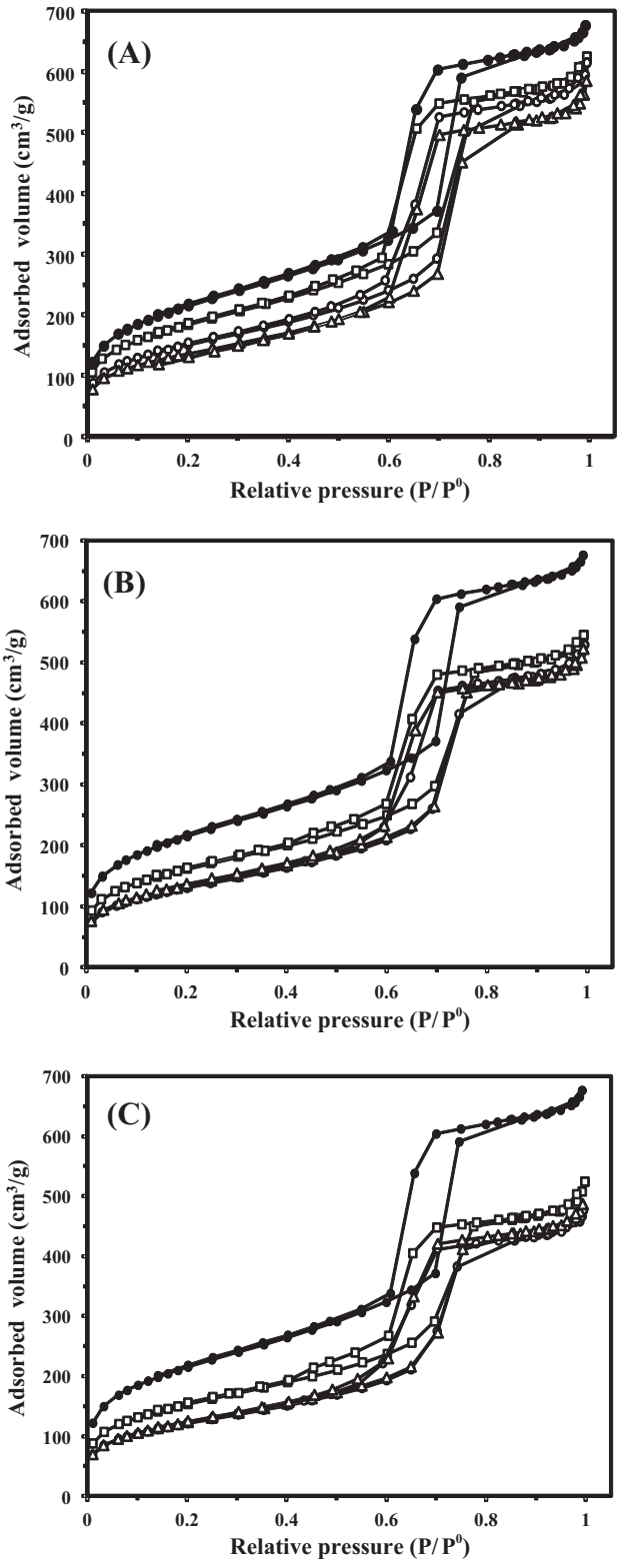

Fig. 1. Nitrogen adsorption–desorption isotherms of ● SBA-15 support, □ CoMo(x), △ CoMo(x)E and ○ CoMo(x)C supported catalysts, (A) $x = 6$, (B) $x = 12$ and (C) $x = 18$.

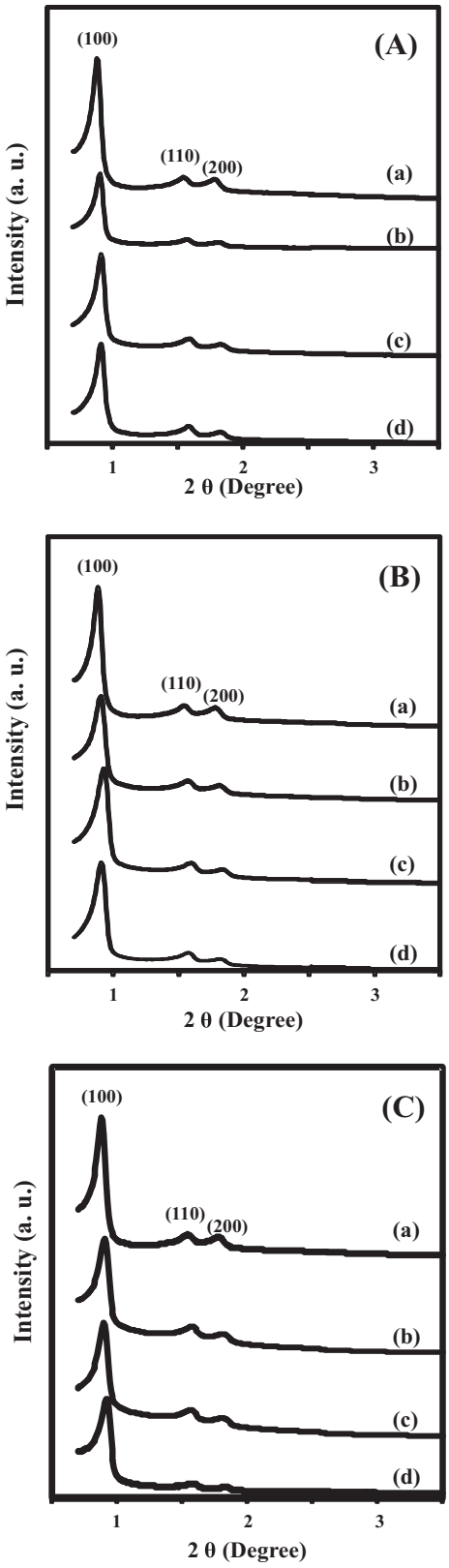

Fig. 2. Small-angle XRD patterns of (a) SBA-15, (b) CoMo(x), (c) CoMo(x)E and (d) CoMo(x)C. Catalysts series (A) $x = 6$, (B) $x = 12$ and (C) $x = 18$.

TPR profiles of the CoMo/SBA-15 catalysts as a consequence of the metal content and the chelating agent used. The CoMo(x)(y) catalysts with the highest metal content showed a similar behavior in the main reduction peak of Mo(VI) species due to the addition of EDTA or CA, pointing out a good dispersion of the catalysts prepared with those chelating agents. The addition of EDTA or CA for preparing these catalysts resulted in a beneficial effect on the reducibility of the Mo(VI) species to diminish the reduction temperature. On the other hand, the CoMo(x) catalysts prepared without chelating agents presented a reduction peak between 600–750 °C

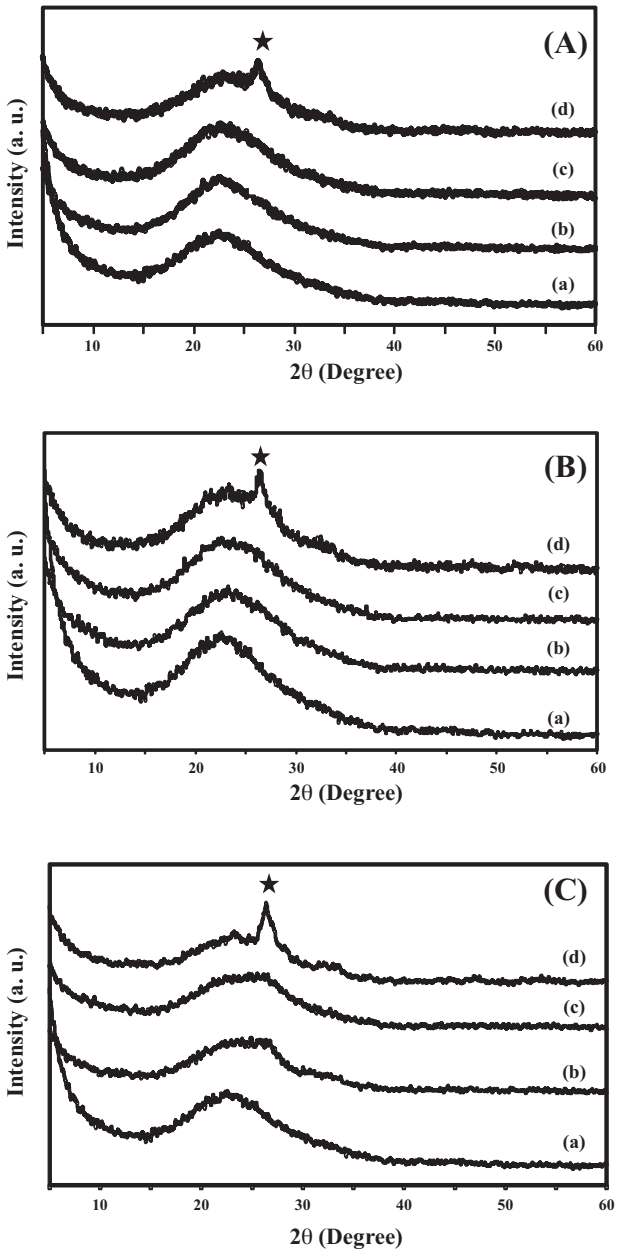

Fig. 3. Powder XRD patterns of (a) SBA-15, (b) CoMo(x)E, (c) CoMo(x)C and (d) CoMo(x). Catalysts series (A) $x = 6$, (B) $x = 12$ and (C) $x = 18$. ⋆ β-$CoMoO_4$ (JCPDS card 21-868).

Table 2
Average length and stacking degree of MoS_2 crystallites in CoMo12(y) catalysts.

Catalyst	Average length (Å)	Average stacking (number of layers)
CoMo12	42	3.1
CoMo12E	35	3.5
CoMo12C	39	3.4

which increases with the metal concentration on the support. This reduction peak at higher temperature can be attributed to the reduction of β-$CoMoO_4$ species detected by powder XRD. The modification on the TPR profiles by the addition of chelating agents showed the increment in the dispersion of metal species supported on SBA-15.

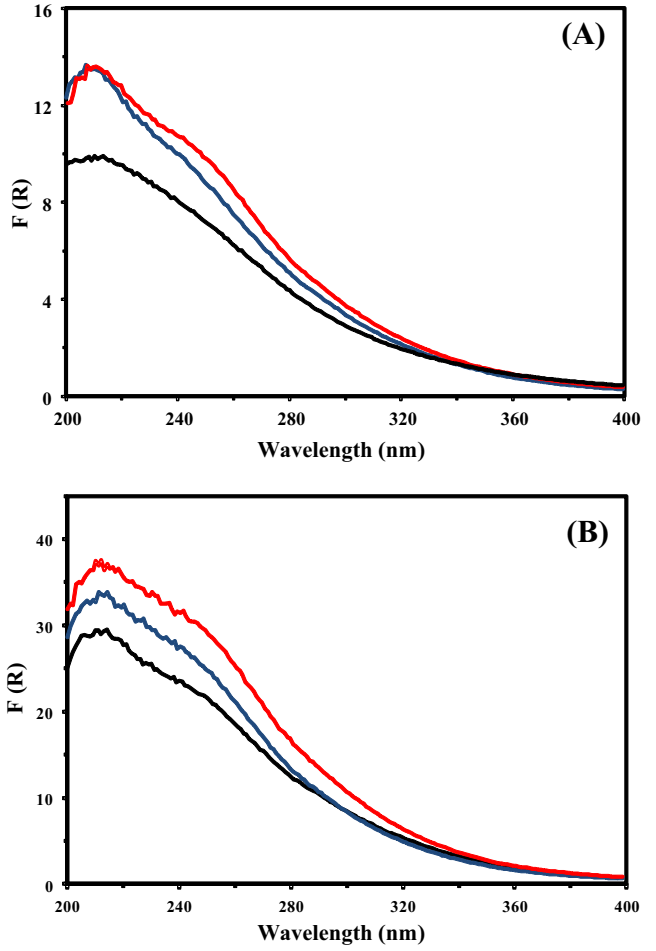

Fig. 4. UV–vis DR spectra ▬ of CoMo(x), ▬ CoMo(x)E and ▬ CoMo(x)C. Catalysts series (A) $x = 6$ and (B) $x = 12$.

HRTEM measurements of CoMo12(y) sulfided catalysts were performed to obtain more information about dispersion of MoS_2 crystallites on SBA-15 by using EDTA and CA in the impregnation solution. Representative micrographs were selected for each of catalysts (Fig. 6), arrows note the MoS_2 crystallites at each micrograph. The micrographs show fringes due to MoS_2 crystallites with 6.1 Å interplanar distances. Distribution of length (Fig. 7) and stacking degree (Fig. 8) was calculated for the CoMo12(y) catalysts. The morphology of MoS_2 crystallites was modified by the EDTA or CA addition in the impregnation solution. CoMo12(y) catalysts have MoS_2 crystallites with a length between 20 Å and 100 Å and stacking degree from one to six layers. The length of MoS_2 crystallites for CoMo12 catalyst has principally MoS_2 particles between 20 Å and 60 Å, while the length distribution of CoMo12E and CoMo12C catalysts have them between 20 Å and 40 Å. The length distribution of CoMo12 catalyst is almost 50% at 21–40 Å, while the ones for CoMo12E and CoMo12C catalysts are around 74% and 69%, respectively. The CoMo12E catalyst exhibited the larger distribution of smaller particles. The use of both chelating agents resulted in a decrease on the length of the MoS_2 catalytically particles supported on SBA-15, pointing out the good dispersion of the sulfided catalysts. On the other hand, the stacking degree of CoMo12 catalyst has a lower number of layers (2–4), while the stacking degree of CoMo12E and CoMo12C results in a higher stacking degree (2–6). Based on the stacking degree distribution of MoS_2 active phase supported on SBA-15, the use of both chelating agents results in a higher staking degree of the sulfided catalysts. Average length and stacking degree of CoMo12(y) sulfided catalysts supported on

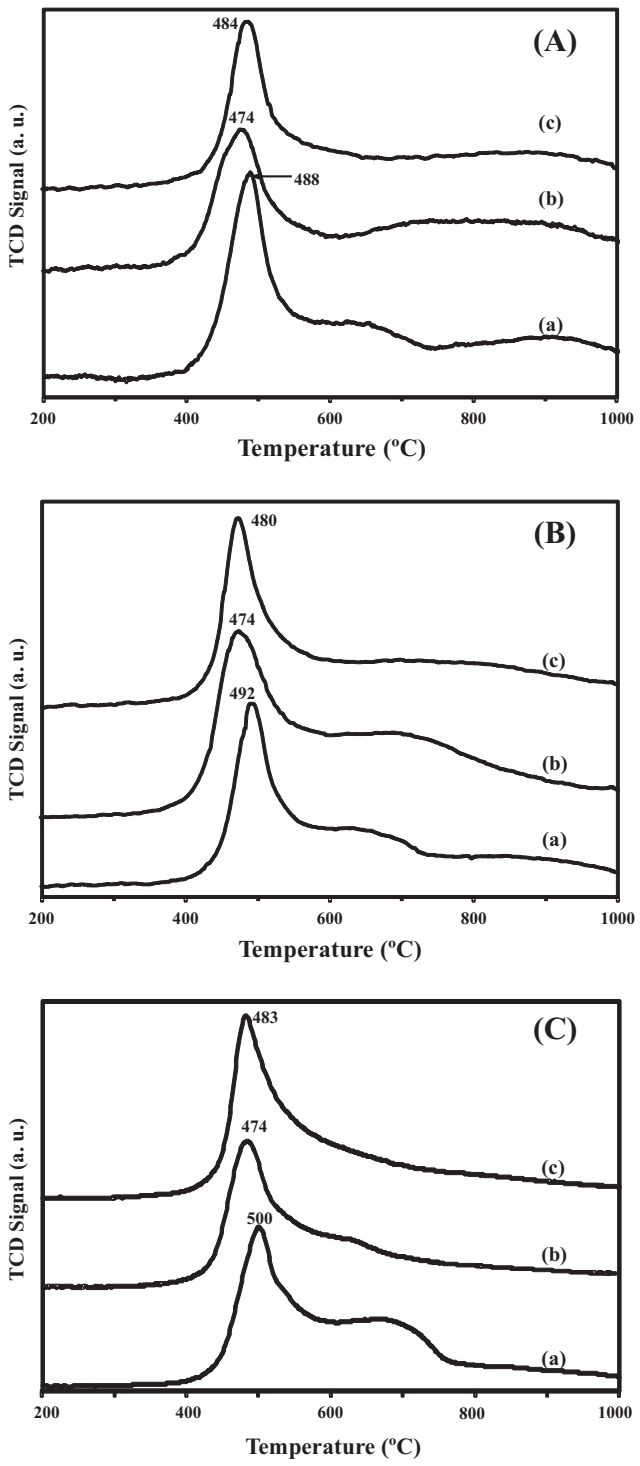

Fig. 5. TPR profiles of (a) CoMo(x), (b) CoMo(x)E and (c) CoMo(x)C. Catalysts series (A) $x = 6$, (B) $x = 12$ and (C) $x = 18$.

SBA-15 are shown in Table 2. CoMo12 catalyst prepared without chelating agents has an average length of 42 Å and an average stacking degree of 3.1. EDTA or CA addition in impregnation solution results in a decrease in the average length and an increase of stacking degree of MoS_2 crystallites. Short MoS_2 particles were formed predominantly in the sulfided CoMo12E and CoMo12C catalysts. CoMo12E catalyst has an average length of 35 Å and a stacking degree of 3.5, whereas the CoMo12C catalyst exhibits an average length of 39 Å and a stacking degree of 3.4.

Table 3
Overall rate constants (k) and conversions at 4 and 8 h in HDS of DBT.

Catalyst	k[a] (mol L^{-1} h^{-1})	k normalized[b] ($mole_{DBT}$ $mole_{Mo}^{-1}$ h^{-1})	DBT conversion (%)	
			4 h[c]	8 h
CoMo6	3.0×10^{-3}	1.92	15.5	37.4
CoMo12	4.2×10^{-3}	1.34	25.2	53.2
CoMo18	4.9×10^{-3}	1.05	30.0	63.0
CoMo6E	5.0×10^{-3}	3.20	33.9	61.9
CoMo12E	6.1×10^{-3}	1.95	38.4	76.5
CoMo18E	7.4×10^{-3}	1.58	47.6	91.6
CoMo6C	3.4×10^{-3}	2.18	22.2	42.8
CoMo12C	4.9×10^{-3}	1.57	30.5	61.5
CoMo18C	6.1×10^{-3}	1.30	35.2	77.4

[a] Pseudo zero-order rate constant.
[b] Pseudo zero-order rate constant expressed as mole of DBT per mole of Mo per h.
[c] Reaction time.

3.2. Catalytic activity

The CoMo catalysts were tested in hydrodesulfurization of DBT. This molecule is commonly used as a model of refractory sulfur-containing compounds present in petroleum [34]. HDS of DBT proceeds through two distinct routes, namely (i) direct desulfurization (DDS) and (ii) hydrogenation (HYD), whose main products are biphenyl (BP) and cyclohexylbenzene (CHB), respectively [35]. A general reaction network for DBT is shown in Fig. 9. The major preference of DBT in its network is dependent of some HDS conditions, specially the nature of the catalyst, such as support composition, active phase, promoter and additive [36–38].

DBT conversions obtained over CoMo catalysts supported on SBA-15 are shown in Table 3. The lowest conversion of DBT was obtained over CoMo catalysts without chelating agents for all the charges studied. The catalytic constants showed the same trend than the conversion (Table 3). It can be seen the increment in HDS activity of CoMo/SBA-15 catalysts when they were prepared with chelating agents. In general, the catalysts prepared with EDTA are more active than the ones prepared with CA. As the metal charge increases in the catalysts, their activity also increases, this effect is related to the larger number of catalytically active sites. However, it is clearly observed that CoMo catalysts prepared without chelating agents exhibited little increment. This effect on CoMo catalysts synthesized without chelating agents is related to the poor dispersion of the active phase on SBA-15. The absence of β-$CoMoO_4$ crystalline phase pointing out the beneficial effect of EDTA or CA during the preparation of CoMo catalysts supported on SBA-15 and the consequences in the catalytic activity is clearly observed. We detected the smaller particles in sulfided catalysts by HRTEM measurements when the metals were impregnated in the presence of EDTA and CA. The highly active catalysts were the ones which exhibited the smaller length particles.

The CoMo/SBA-15 catalysts prepared with EDTA are more active than those prepared with CA. These results can be related to the coordination compounds in the impregnation solution between cobalt and each of chelating agent. EDTA produces hexacoordinate structures, while CA produces tricoordinate ones in aqueous solutions. In the present preparation conditions, we maintained a stoichiometry to form hexacoordinate inorganic compounds (Co:EDTA = 1:1 and Co:CA = 1:2), thus the Co(II) complex with an octahedral symmetry was synthesized in aqueous solution with each chelating agent. However, EDTA is a stronger chelating agent because it has six atoms in one molecule to bind the metal atom and the CA has three ones. The replacement of these organic ligands by the support is not the same. The chelate effect of EDTA is much higher than the corresponding with CA. These differences in the EDTA and CA structures and their related Co(II) complexes in

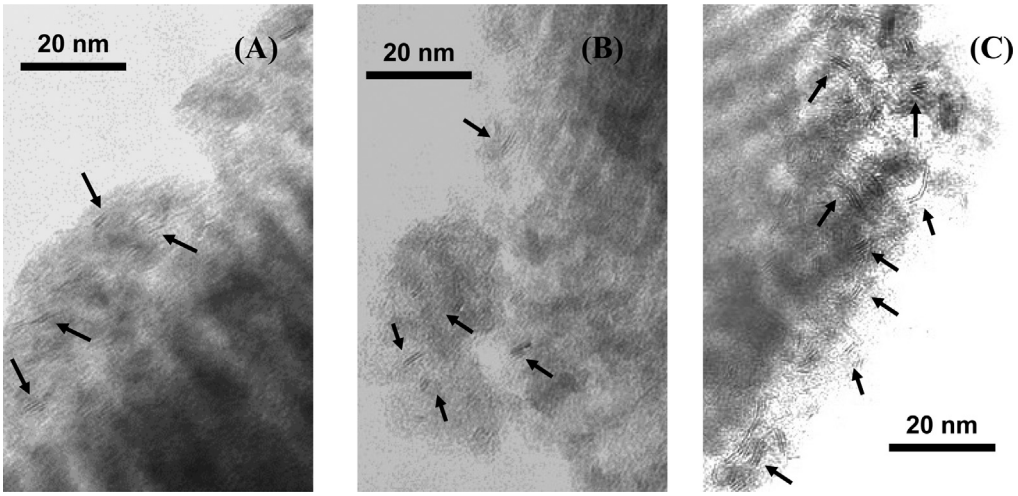

Fig. 6. HRTEM micrographs of sulfided catalysts: (A) CoMo12, (B) CoMo12E and (C) CoMo12 C.

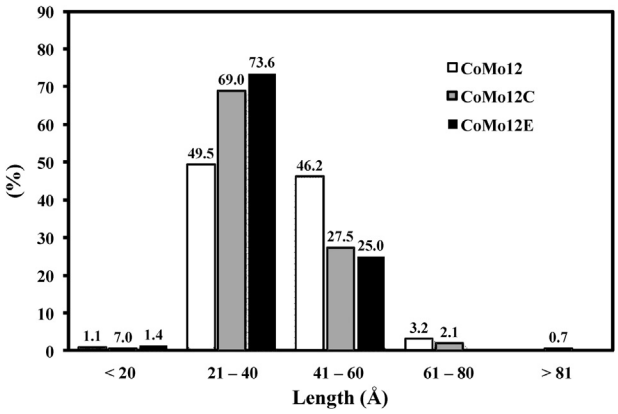

Fig. 7. Length distributions of MoS_2 crystallites in sulfided CoMo12(y) catalysts supported on SBA-15.

the impregnation solution can be the responsible for the catalytic performance.

The use of both chelating agents provides a good strategy to improve the catalytic activity of CoMo catalysts supported on SBA-15. As we mentioned above, some experiments have been performed to modify the composition of silica-based supports, they are typically focused on the oxides incorporation to increase the metal dispersion. The silica modification with oxides such as ZrO_2 and TiO_2 has shown better dispersion than the catalysts supported on pure silica and the β-$CoMoO_4$ crystalline phase is avoided [6–8]. The results in this work have some advantages because the preparation of catalysts does not require several steps. The impregnation of the metal species to the SBA-15 proceeds in only one step and the catalysts are highly active in HDS.

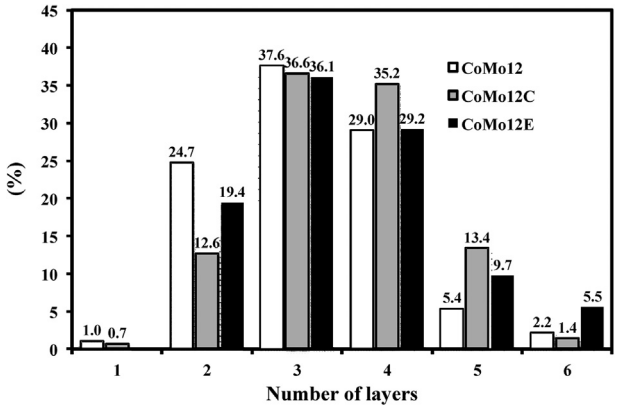

Fig. 8. Layer stacking distributions of MoS_2 crystallites in sulfided CoMo12(y) catalysts supported on SBA-15.

The assumption that catalysts prepared with chelating agents should not be calcined before sulfidation stage has been a true fact for HDS catalysts supported on γ-Al_2O_3 or other typical supports [11,14–21]. However, the MoS_2-based catalysts supported on SBA-15 showed better performance in HDS of dibenzothiophene-type compounds when they were calcined [24,39]. Moreover, other catalytic system using chelating agents exhibited an enhancement in their performance when they were calcined [12]. We point out that addition of EDTA or CA affects the interaction between metals and support during impregnation stage, when the catalysts were dried, metals were deposited on the support and the dispersion was also maintained after calcination at 500 °C because the metal–support interactions occurred at liquid–solid interface. Our HDS results have confirmed the complexity of the addition of EDTA or CA in the impregnation solution and their particular treatment of each support.

Selectivity modifications in HDS of DBT over these catalysts were analyzed to gain more insight into the effect of EDTA or CA addition in the CoMo catalysts supported on SBA-15. Selectivity changes in HDS of DBT over each catalyst due to EDTA and CA addition can also be appreciated in distribution of BP and CHB compounds, the main products of DDS and HYD routes, respectively. The composition of products was analyzed at 30% DBT conversion (Table 4). It can be observed differences in the products in HDS of DBT. In general, HDS of DBT over these catalysts proceed toward the DDS route. However, we noted that the catalysts prepared with chelating agents resulted in the larger composition of the CHB product, the main product of the HYD route. The BP/CHB ratio which is directly related to the DDS/HYD ratio exhibited a decrease in the following order: CoMo(x)E < CoMo(x)C < CoMo(x) for all of the metal charges studied. As we mentioned above, the catalysts prepared with EDTA and CA showed larger stacking degree than the ones prepared without chelating agents. The DDS/HYD ratio obtained in HDS of DBT over the more stacked catalysts is in good agreement. Moreover, the thermodynamic stability of HYD route is larger than its DDS counterpart [40], the selectivity preference of these catalysts could also explain the activity observed because DBT reacts

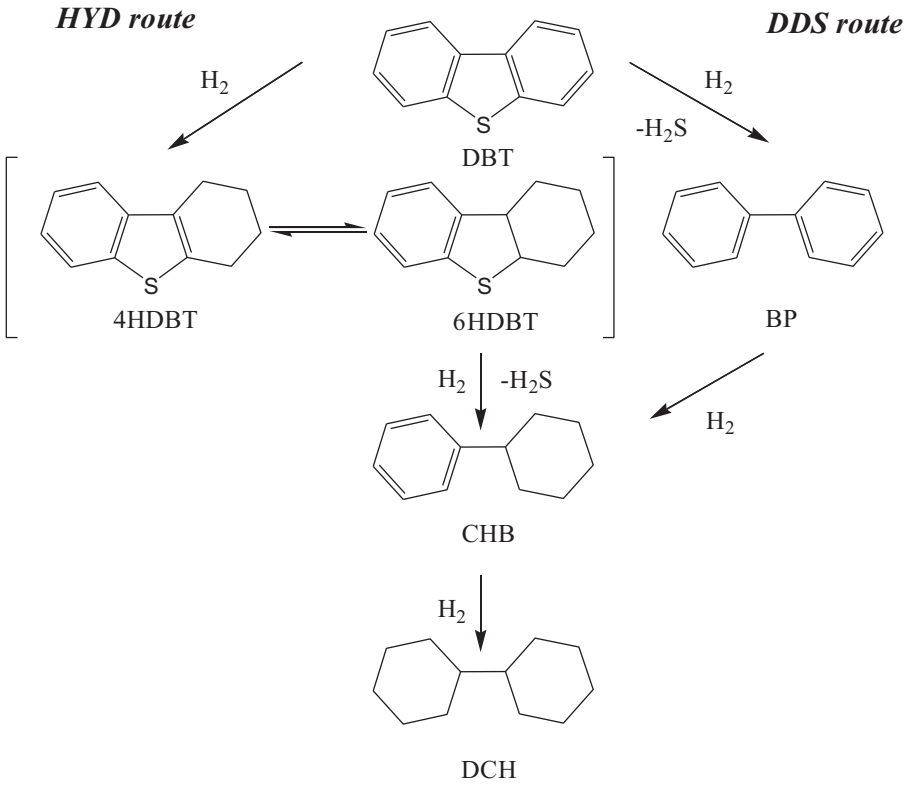

Fig. 9. Reaction network for hydrodesulfurization of DBT.

Table 4
Composition of products obtained over CoMo/SBA-15 catalysts (at 30% of DBT conversion).

Catalyst	Products (%)[a]				
	4HDBT	BP	CHB	DCH	BP/CHB
CoMo6	4.6	70.0	24.6	0.8	2.84
CoMo12	5.0	67.0	27.5	0.5	2.44
CoMo18	4.9	62.9	31.4	0.8	2.00
CoMo6E	0.0	66.9	32.2	0.9	2.07
CoMo12E	0.0	63.1	36.1	0.8	1.75
CoMo18E	0.0	62.4	36.8	0.8	1.69
CoMo6C	4.6	65.2	29.5	0.7	2.21
CoMo12C	3.1	65.2	30.9	0.8	2.11
CoMo18C	0.8	65.2	33.3	0.7	1.95

[a] 4HDBT = tetrahydrodibenzothiophene; BP = biphenyl; CHB = cyclohexylbenzene; DCH = dicyclohexyl.

toward DDS route in a minor proportion over the highly active catalysts.

Both chelating agents improve the dispersion of metal species on the SBA-15, as a consequence we observed that catalytic activity increases. EDTA or CA addition in the impregnation solution enhances the catalytic activity for the metal charges studied. Apart from the dispersion of the metal species on SBA-15 support, the selectivity was also modified due to the chelating agents addition in the impregnation solution. We observed the catalysts prepared with EDTA resulted in the smaller values in the BP/CHB ratio compared to the ones prepared with CA. The larger preference of these catalysts toward HYD route can also explain their catalytic performance because the CoMo(x)C catalysts exhibited also good dispersion. The CoMo(x)E catalysts were the highly active because their selectivity had the largest preference toward HYD route for all the CoMo(x)(y) catalysts studied.

4. Conclusions

CoMo catalysts supported on SBA-15 were synthesized with EDTA and CA, varying their metal charges. According to the characterization results, the preparation procedure maintains the SBA-15 template characteristics. CoMo catalysts prepared without chelating agents showed the presence of the β-$CoMoO_4$ crystalline phase. Chelating agents avoided the formation of this crystalline phase. The morphology of the active phase was modified when the chelating agents were added. Furthermore, the addition of EDTA and CA in the impregnation solutions results in better dispersion of metal species in the SBA-15 support. The catalysts prepared with chelating agents were much higher active than their counterparts prepared without them. EDTA and CA allow better use of metal charges in the CoMo catalysts supported on SBA-15. The catalysts prepared with EDTA were the highly active for all the metal charges studied. DBT reacts preferably trough DDS route for all the catalysts. However, DBT reacts over the highly active catalysts with a minor proportion trough the DDS route.

Acknowledgements

Financial support by CONACyT-Mexico (grant 100945) is gratefully acknowledged. The authors thank C. Salcedo Luna, M. Aguilar and I. Puente Lee for technical assistance with powder and small-angle XRD and electron microscopy characterizations, respectively.

References

[1] C.-M. Fu, A.M. Schaffer, Ind. Eng. Chem. Prod. Res. Dev. 24 (1985) 68–75.
[2] E. Furimsky, Appl. Catal. A 199 (2000) 147–190.
[3] D. Valencia, T. Klimova, I. García-Cruz, Fuel 100 (2012) 177–185.
[4] A. Stanislaus, A. Marafi, M.S. Rana, Catal. Today 153 (2010) 1–68.
[5] E.J.M. Hensen, P.J. Kooyman, Y. van der Meer, A.M. van der Kraan, V.H.J. de Beer, J.A.R. van Veen, R.A. van Santen, J. Catal. 199 (2001) 224–235.

[6] D. Valencia, T. Klimova, Catal. Today 166 (2011) 91–101.
[7] R. Nava, B. Pawelec, J. Morales, R.A. Ortega, J.L.G. Fierro, Microporous Mesoporous Mater. 118 (2009) 189–201.
[8] R. Nava, R.A. Ortega, G. Alonso, C. Ornelas, B. Pawelec, J.L.G. Fierro, Catal. Today 127 (2007) 70–84.
[9] J. Brito, L. Barbosa, J. Catal. 171 (1997) 467–475.
[10] R. Cattaneo, T. Shido, R. Prins, J. Catal. 185 (1999) 199–212.
[11] K. Hiroshima, T. Mochizuki, T. Honma, T. Shimizu, M. Yamada, Appl. Surf. Sci. 121/122 (1997) 433–436.
[12] P. Mazoyer, C. Geantet, F. Diehl, S. Loridant, M. Lacroix, Catal. Today 130 (2008) 75–79.
[13] M.A. Leilas, E. Le Guludec, L. Mariey, J. van Gestel, A. Travert, L. Oliviero, F. Maugé, Catal. Today 150 (2010) 179–185.
[14] P. Castillo-Villalón, J. Ramírez, R. Castañeda, J. Catal. 294 (2012) 54–62.
[15] K. Al-Dalama, A. Stanislaus, Energy Fuels 20 (2006) 1777–1783.
[16] M.S. Rana, J. Ramírez, A. Gutiérrez-Alejandre, J. Ancheyta, L. Cedeño, S.K. Maity, J. Catal. 246 (2007) 100–108.
[17] M.A. Lélias, P.J. Kooyman, L. Mariey, L. Oliviero, A. Travert, J. van Gestel, J.A.R. van Veen, F. Maugé, J.Catal. 267 (2009) 14–23.
[18] T. Fujikawa, Top. Catal. 52 (2009) 872–879.
[19] T. Fujikawa, M. Kato, T. Ebihara, K. Hagiwara, T. Kubota, Y. Okamoto, J. Jpn. Petrol. Inst. 48 (2005) 114–120.
[20] T. Fujikawa, M. Kato, T. Ebihara, K. Hagiwara, T. Kubota, Y. Okamoto, J. Jpn. Petrol. Inst. 48 (2005) 106–113.
[21] N. Rinaldi, T. Kubota, Y. Okamoto, Ind. Eng. Chem. Res. 48 (2009) 10414–10424.
[22] D. Valencia, I. García-Cruz, T. Klimova, Stud. Surf. Sci. Catal. 175 (2010) 529–532.
[23] S. Badoga, K.C. Moulia, K.K. Sonia, A.K. Dalai, J. Adjay, Appl. Catal. B: Environ. 125 (2012) 67–84.
[24] D. Valencia, T. Klimova, Catal. Commun. 21 (2012) 77–81.
[25] D. Valencia, T. Klimova, Appl. Catal. B: Environ. 129 (2013) 137–145.
[26] D. Zhao, J. Feng, Q. Huo, N. Melosh, G.H. Fredrickson, B.F. Chmelka, G.D. Stucky, Science 279 (1998) 548.
[27] D. Zhao, Q. Huo, J. Feng, B.F. Chmelka, G.D. Stucky, J. Am. Chem. Soc. 120 (1998) 6024–6036.
[28] J. Escobar, M.C. Barrera, J.A. de los Reyes, J.A. Toledo, V. Santes, J.A. Colín, J. Mol. Catal. A. Chem. 287 (2008) 33–40.
[29] T. Yamada, H. Zhou, K. Asai, I. Honma, Mater. Lett. 56 (2002) 93–96.
[30] A. Infantes-Molina, J. Mérida-Robles, E. Rodríguez-Castellón, J.L.G. Fierro, A. Jiménez-López, J. Catal. 240 (2006) 258–267.
[31] R.I. Maksimovskaya, G.M. Maksimov, Inorg. Chem. 46 (2007) 3688–3695.
[32] R.S. Weber, J. Catal. 151 (1995) 470–474.
[33] R. López Cordero, A. López Agudo, Appl. Catal. A 202 (2000) 23–35.
[34] B.C. Gates, H. Tøpsoe, Polyhedron 16 (1997) 3213.
[35] M.J. Girgis, B.C. Gates, Ind. Eng. Chem. Res. 30 (1991) 2021–2058.
[36] H. Wang, R. Prins, J. Catal. 264 (2009) 31–43.
[37] T. Klimova, L. Peña, L. Lizama, C. Salcedo, O.Y. Gutiérrez, Ind. Eng. Chem. Res. 48 (2009) 1126–1133.
[38] H. Farag, D.D. Whitehurst, K. Sakanishi, I. Mochida, Catal. Today 50 (1999) 49–56.
[39] T. Klimova, D. Valencia, J. Mendoza, P. Hipolito, J. Catal. 304 (2013) 29–46.
[40] D. Valencia, L. Peña, I. García-Cruz, Int. J. Quantum Chem. 112 (2012) 3599–3605.